

# Quadristor: a novel device for superconducting electronics

Sara Chahid, Serafim Teknowijoyo, and Armen Gulian\*  
*Advanced Physics Laboratory, Institute for Quantum Studies,  
 Chapman University, Burtonsville, MD 20866, USA*  
 (Dated: November 28, 2022)

We designed and experimentally demonstrated a four-terminal superconducting device which can function as a non-latching (reversible) superconducting switch from the diode regime to the resistive state by applying a control current much smaller than the main transport current. The device utilizes a vortex-based superconducting diode mechanism which is switched back and forth via the injection of flux quanta through auxiliary current leads. Various applications in superconducting electronics can be foreseen.

Simultaneous breaking of time reversal symmetry and inversion symmetry generates the superconducting diode effect [1–8]. The time reversal symmetry could be broken via an externally applied magnetic field or internal inclusions of magnetic micro-clusters, while the inversion symmetry could be broken in several ways: [4, 6, 9–22].

The recent spike of research in the area of superconducting diodes is paving a road towards the future practical application of these novel devices in superconducting electronics. Moreover, it inspires substantiated hopes that the next stages of work, in analogy with semiconductor electronics, will be accomplished by developing superconducting transistors. By a “transistor” we refer to a regulated diode, whose resistive state can be controlled by an externally applied signal exerting much less power than the one it controls. In this report, we introduce such a device. Because of the specifics of superconductivity, where the devices are current-biased, the controlling agent in our design is a current supplied by two auxiliary leads. This justifies the term “quadristor”: two leads for the transport and two leads for the control currents. Via this relatively small control current, the diode effect can be turned off and on by demand without noticeable latching effect and can function as a fast switch or as a signal controller/amplifier.

We used  $\text{Nb}_3\text{Sn}$  films on sapphire substrates with  $T_c > 17$  K, Fig. 1.

The device was fabricated by a multistage lithographic patterning process described in Fig. 2 (the details of deposition and lithography patterning are described elsewhere [22]).

Ion milling affects the physical properties of bridges and reduces the critical temperatures (see. e.g., [19, 22]). In the current case, the bridge had  $T_c \sim 4$  K (Fig. 1).

As was reported previously [22], the bridges prepared in this manner demonstrate a noticeable critical current difference  $\Delta I = I^+ - I^-$ . For the bridge under study, we reached  $\Delta I = 0.5$  mA at  $T = 2$  K and  $H = 50$  Oe (Fig. 3; similarly with [19, 22], at positive values of applied magnetic field,  $I^+ < I^-$  and vice versa) with very robust diode effect (Fig. 4).

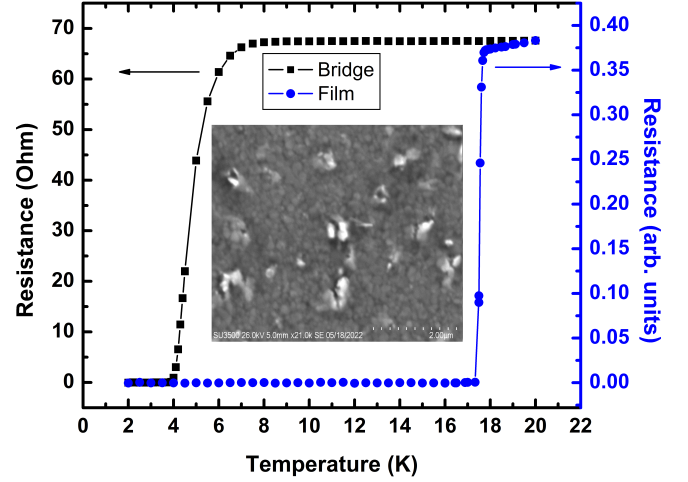


FIG. 1. Superconducting resistive transition in our  $\text{Nb}_3\text{Sn}$  film and the processed bridge from it. Resistive transition of the bridge shows reduction of  $T_c$  (in this work, we did not attempt its restoration to 17 K by annealing as we did in our previous work [22] and used the bridge as prepared). SEM image (inset) shows the material’s granularity with the average grain size about 200 nm, as well as larger in size nanomountains which, as the EDX revealed, contain excess amount of Sn (further information about the latter could be obtained in [22]).

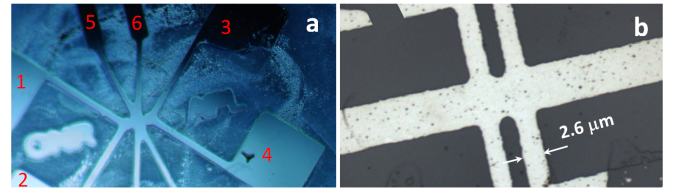


FIG. 2. Consecutive steps in lithographic processing of the device. (a) Larger scale pattern obtained after 3D-printing and ion milling; numeric labels indicate contact pads (two more of them, 7 and 8 are not shown); the lateral size of the bridge is  $\approx 100$   $\mu\text{m}$ . (b) Final layout of the central part of the bridge after projection photolithography and ion milling. The projection mask had nanoholes which transferred onto the  $\text{Nb}_3\text{Sn}$  material. Their role will be discussed further in the text.

\* Corresponding author: gulian@chapman.edu

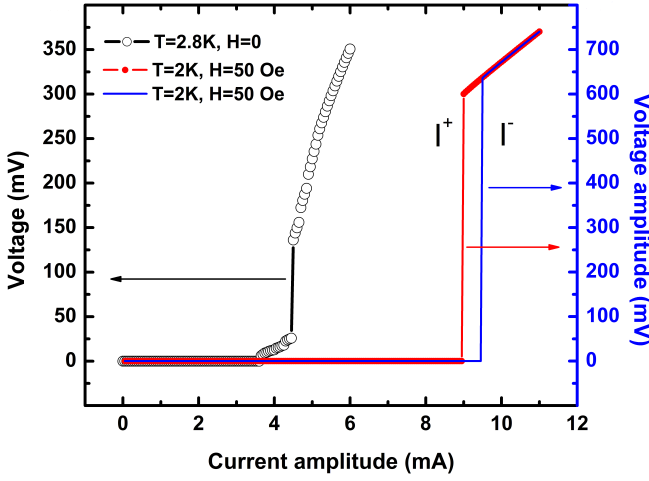


FIG. 3. Voltage-current curve (measured by Quantum Design PPMS system) at 2.8 K and  $H = 0$  demonstrates steps caused by certain re-structuring of vortex patterns in the bridge [19, 22–25]. Voltage-current characteristics (measured by Keithley 6221 current source and 2182A nanovoltmeter) at  $T = 2$  K in the PPMS cryostat at  $H = 50$  Oe (at this and all other measurements reported in this article, the direction of  $\mathbf{H}$  is orthogonal to the surface of the film) at positive and negative directions of the dc current flow.

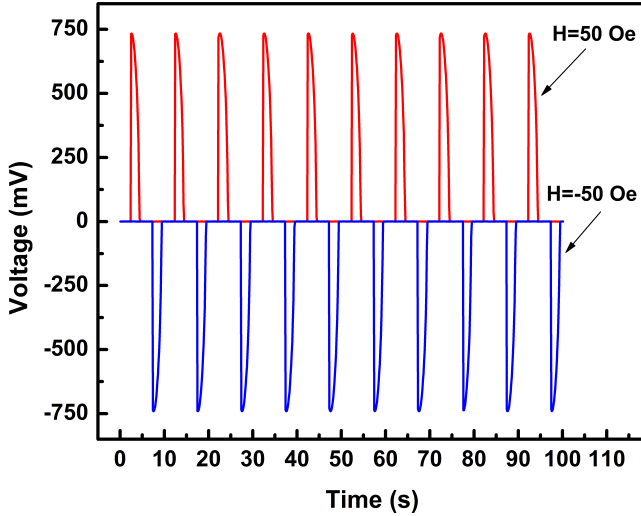


FIG. 4. Diode effect at usual four-probe connection of the bridge: current is applied via contacts 1 and 3, and voltage is measured between contacts 2 and 4 (see Fig. 2a) at positive and negative external magnetic fields at  $T = 2$  K.

It is worth mentioning that the existence of nanoholes displayed in Fig. 2b creates an analogy between this diode behavior and the one mentioned in Ref. [26] where the conformally mapped holes were artificially introduced in a homogeneous superconducting strip to break the inversion symmetry. In our case, the inhomogeneously populated nanoholes exist as a consequence of photo-projection mask imperfections which are inevitable at

the laser printing technique used for the mask preparation, and unexpectedly caused a positive impact. This, however, needs more studies, since, as mentioned in [19, 21, 22], the edge imperfections can also facilitate the inversion symmetry breaking.

The main idea of the quadristor design stemmed from a hypothesis that the underlying mechanism of this diode effect is based on vortex lattice dynamics in the active area of the bridge. The additional leads (the pairs 5, 6 and 7, 8) attached to that area were added for seeding vortices in the laminar flow of supercurrent, thus triggering major vortex pattern (turbulence) generation. The intuitive belief that this external triggering should work has been indeed experimentally confirmed (Fig. 5): the diode effect via leads 1 – 4 is replaced by a resistive state when the auxiliary current through the leads 5 and 6 is  $On$  (this numbering corresponds to that in Fig. 2a). The prediction that there would be no latching was much less obvious. However, the removal of the current through these auxiliary leads restored the laminar flow at diode performance, as Fig. 5 demonstrates. Predictably, a similar result occurs when one uses the other two auxiliary leads (7 and 8) for the control current.

The device performance resembles that of the planar transistor-type devices suggested recently in multiple articles. However, in these devices, the design is based on different principles, for example, the field-effect, which modifies the density of states, or the injection of high-energy electrons, which generates nonequilibrium phonon fluxes, etc. These approaches require the application of potentials in the eV range, which is above the intrinsic characteristic energy scale of superconductors (meV). The controlling current of our quadristor is significantly smaller than the transport current through it, so our device can be effectively used in circuits of superconducting microelectronics, such as logical elements, amplifiers, etc.

In conclusion, we experimentally demonstrated a newly suggested design of current-controlled four-terminal device which reversibly switches the superconducting diode into a resistive state and back. The mechanism of switching is based on nonequilibrium kinetics of vortices in the active area of the device. Since the dioding is also based on this mechanism and the high-frequency operation is demonstrated for it [22], there are reasons to expect that switching will also be possible at high-frequencies.

The aim of this research was to prove the operational principle of the device. Importantly, the control current ( $I_{ctr} = 2.5$  mA) is much smaller than the amplitude of the ac transport current ( $I_{tr} = 9.25$  mA). At further optimization of the quadristor parameters, the gain  $g = I_{tr}/I_{ctr}$  may be further enhanced. However, even with the currently achieved gain,  $g = 3 - 4$ , the quadristor can serve as a signal amplifier. Moreover, the transport current through it can be controlled by many switches (two in our current design). Thus, our development opens opportunities for various applications in true (non-hybrid) superconducting microelectronics, in-

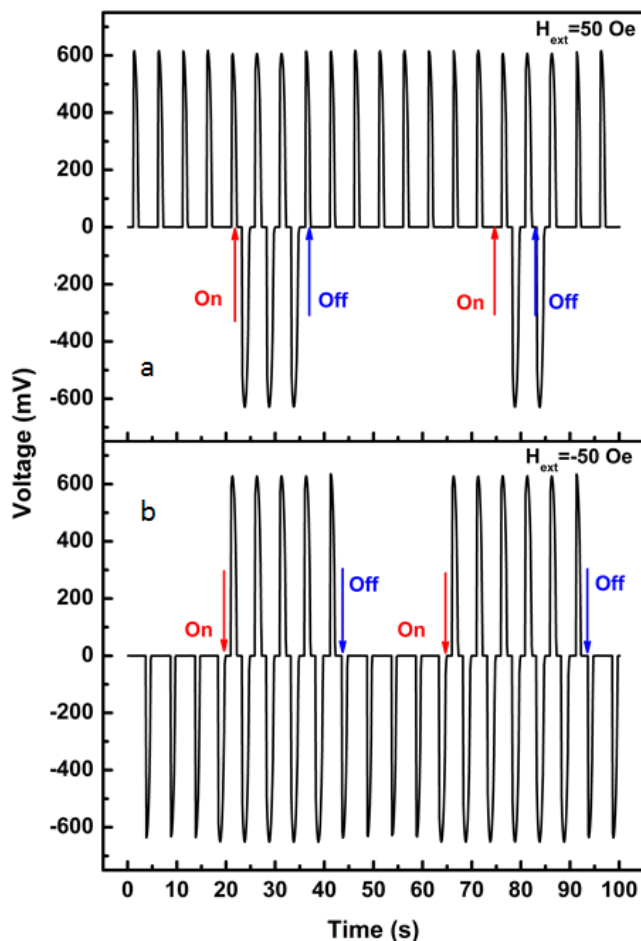


FIG. 5. Performance of quadristor at application of the control current. The transport current measurements were performed at  $T = 2$  K via main leads 1 – 4, while the control current was supplied via auxiliary leads 5, 6 or 7, 8 (see Fig. 2a for details). As in Fig. 4, the amplitude and frequency of the ac transport current were 9.25 mA (a choice dictated by results presented in Fig. 3) and 0.2 Hz correspondingly. The control dc current was 2.5 mA (supplied by Keithley 220 current source). The arrows indicate moments of time when the control current was switched *On* and *Off*. Panels (a) and (b) correspond to positive and negative external fields  $H = \pm 50$  Oe, similar to Fig. 4.

cluding logical units in leading-edge quantum information tasks. It also opens novel opportunities for exploration of fundamental problems of non-equilibrium states of superconductors and turbulent-laminar motion interplay in superfluid liquids.

This work is supported by the ONR grants N00014-21-1-2879 and N00014-20-1-2442.

- 
- [1] Y. Tokura and N. Nagaosa, Nonreciprocal responses from non-centrosymmetric quantum materials, *Nature Communications* **9**, 3740 (2018).
  - [2] R. Wakatsuki and N. Nagaosa, Nonreciprocal Current in Noncentrosymmetric Rashba Superconductors, *Phys. Rev. Lett.* **121**, 026601 (2018).
  - [3] S. Hoshino, R. Wakatsuki, K. Hamamoto, and N. Nagaosa, Nonreciprocal charge transport in two-dimensional noncentrosymmetric superconductors, *Phys. Rev. B* **98**, 054510 (2018).
  - [4] F. Ando, Y. Miyasaka, T. Li, J. Ishizuka, T. Arakawa, Y. Shiota, T. Moriyama, Y. Yanase, and T. Ono, Observation of superconducting diode effect, *Nature* **584**, 373 (2020).
  - [5] T. Ideue and Y. Iwasa, One-way supercurrent achieved in an electrically polar film, *Nature* **584**, 349 (2020).
  - [6] C. Baumgartner, L. Fuchs, A. Costa, S. Reinhardt, S. Gronin, G. C. Gardner, T. Lindemann, M. J. Manfra, P. E. Faria Junior, D. Kochan, J. Fabian, N. Paradiso, and C. Strunk, Supercurrent rectification and magnetochiral effects in symmetric Josephson junctions, *Nature Nanotechnology* **17**, 39 (2022).
  - [7] H. Wu, Y. Wang, Y. Xu, P. K. Sivakumar, C. Pasco, U. Filippozzi, S. S. P. Parkin, Y.-J. Zeng, T. McQueen,

- and M. N. Ali, The field-free Josephson diode in a van der Waals heterostructure, *Nature* **604**, 653 (2022).
- [8] E. Strambini, M. Spies, N. Ligato, S. Ilić, M. Rouco, C. González-Orellana, M. Ilyn, C. Rogero, F. S. Bergeret, J. S. Moodera, P. Virtanen, T. T. Heikkilä, and F. Giazotto, Superconducting spintronic tunnel diode, *Nature Communications* **13**, 2431 (2022).
- [9] N. F. Q. Yuan and L. Fu, Supercurrent diode effect and finite-momentum superconductors, *Proceedings of the National Academy of Sciences* **119**, e2119548119 (2022).
- [10] S. Ilić and F. S. Bergeret, Theory of the Supercurrent Diode Effect in Rashba Superconductors with Arbitrary Disorder, *Phys. Rev. Lett.* **128**, 177001 (2022).
- [11] A. Daido, Y. Ikeda, and Y. Yanase, Intrinsic Superconducting Diode Effect, *Phys. Rev. Lett.* **128**, 037001 (2022).
- [12] T. Karabassov, I. V. Bobkova, A. A. Golubov, and A. S. Vasenko, Hybrid helical state and superconducting diode effect in S/F/TI heterostructures, *arXiv.2203.15608* (2022).
- [13] J. J. He, Y. Tanaka, and N. Nagaosa, A phenomenological theory of superconductor diodes, *New Journal of Physics* **24**, 053014 (2022).
- [14] L. Bauriedl, C. Bäuml, L. Fuchs, C. Baumgartner, N. Paulik, J. M. Bauer, K.-Q. Lin, J. M. Lupton, T. Taniguchi, K. Watanabe, C. Strunk, and N. Paradiso, Supercurrent diode effect and magnetochiral anisotropy in few-layer NbSe<sub>2</sub>, *Nature Communications* **13**, 4266 (2022).
- [15] R. Wakatsuki, Y. Saito, S. Hoshino, Y. M. Itahashi, T. Ideue, M. Ezawa, Y. Iwasa, and N. Nagaosa, Nonreciprocal charge transport in noncentrosymmetric superconductors, *Science Advances* **3**, e1602390 (2017).
- [16] J. Shin, S. Son, J. Yun, G. Park, K. Zhang, Y. J. Shin, J.-G. Park, and D. Kim, Magnetic Proximity-Induced Superconducting Diode Effect and Infinite Magnetoresistance in van der Waals Heterostructure, *arXiv.2111.05627* (2021).
- [17] C. Baumgartner, L. Fuchs, A. Costa, J. Picó-Cortés, S. Reinhardt, S. Gronin, G. C. Gardner, T. Lindemann, M. J. Manfra, P. E. F. Junior, D. Kochan, J. Fabian, N. Paradiso, and C. Strunk, Effect of Rashba and Dresselhaus spin-orbit coupling on supercurrent rectification and magnetochiral anisotropy of ballistic Josephson junctions, *Journal of Physics: Condensed Matter* **34**, 154005 (2022).
- [18] Y. Hou, F. Nichele, H. Chi, A. Lodesani, Y. Wu, M. F. Ritter, D. Z. Haxell, M. Davydova, S. Ilić, F. S. Bergeret, A. Kamra, L. Fu, P. A. Lee, and J. S. Moodera, Ubiquitous Superconducting Diode Effect in Superconductor Thin Films, *arXiv.2205.09276* (2022).
- [19] D. Suri, A. Kamra, T. N. G. Meier, M. Kronseder, W. Belzig, C. H. Back, and C. Strunk, Non-reciprocity of vortex-limited critical current in conventional superconducting micro-bridges, *Applied Physics Letters* **121**, 102601 (2022).
- [20] M. K. Hope, M. Amundsen, D. Suri, J. S. Moodera, and A. Kamra, Interfacial control of vortex-limited critical current in type-II superconductor films, *Phys. Rev. B* **104**, 184512 (2021).
- [21] D. Y. Vodolazov and F. M. Peeters, Superconducting rectifier based on the asymmetric surface barrier effect, *Phys. Rev. B* **72**, 172508 (2005).
- [22] S. Chahid, S. Teknowijoyo, I. Mowgood, and A. Gulian, Diode effect in superconducting Nb<sub>3</sub>Sn micro-bridges at high frequencies, *arXiv.2211.11537* (2022).
- [23] G. R. Berdiyev, A. K. Elmurodov, F. M. Peeters, and D. Y. Vodolazov, Finite-size effect on the resistive state in a mesoscopic type-II superconducting stripe, *Phys. Rev. B* **79**, 174506 (2009).
- [24] P. Sánchez-Lotero, J. Albino Aguiar, and D. Domínguez, Behavior of the flux-flow resistivity in mesoscopic superconductors, *Physica C: Superconductivity and its Applications* **503**, 120 (2014).
- [25] D. Y. Vodolazov and F. M. Peeters, Rearrangement of the vortex lattice due to instabilities of vortex flow, *Phys. Rev. B* **76**, 014521 (2007).
- [26] Y.-Y. Lyu, J. Jiang, Y.-L. Wang, Z.-L. Xiao, S. Dong, Q.-H. Chen, M. V. Milošević, H. Wang, R. Divan, J. E. Pearson, P. Wu, F. M. Peeters, and W.-K. Kwok, Superconducting diode effect via conformal-mapped nanoholes, *Nature Communications* **12**, 2703 (2021).
- [27] M. F. Ritter, A. Fuhrer, D. Z. Haxell, S. Hart, P. Gumann, H. Riel, and F. Nichele, A superconducting switch actuated by injection of high-energy electrons, *Nature Communications* **12**, 1266 (2021).
- [28] M. F. Ritter, N. Crescini, D. Z. Haxell, M. Hinderling, H. Riel, C. Bruder, A. Fuhrer, and F. Nichele, Out-of-equilibrium phonons in gated superconducting switches, *Nature Electronics* **5**, 71 (2022).
- [29] G. De Simoni, F. Paolucci, P. Solinas, E. Strambini, and F. Giazotto, Metallic supercurrent field-effect transistor, *Nature Nanotechnology* **13**, 802 (2018).
- [30] J. Chiles, E. G. Arnault, C.-C. Chen, T. F. Q. Larson, L. Zhao, K. Watanabe, T. Taniguchi, F. Amet, and G. Finkelstein, Non-Reciprocal Supercurrents in a Field-Free Graphene Josephson Triode, *arXiv.2210.02644* (2022).
- [31] M. Gupta, G. V. Graziano, M. Pendharkar, J. T. Dong, C. P. Dempsey, C. Palmström, and V. S. Pribiag, Superconducting Diode Effect in a Three-terminal Josephson Device, *arXiv.2206.08471* (2022).
- [32] F. Paolucci, G. De Simoni, and F. Giazotto, A gate- and flux-controlled supercurrent diode, *arXiv.2211.12127* (2022).